Journal of Mineralogical and Petrological Sciences, Volume 98, page 31-40, 2003

^{57}Fe Mössbauer and X-ray Rietveld studies of ferrian prehnite from Kouragahana, Shimane Peninsula, Japan

Masahide AKASAKA*, Hideaki HASHIMOTO*, Kuniaki MAKINO** and Ryozi HINO***

**Department of Geoscience, Interdisciplinary Faculty of Science and Engineering, Shimane University, 1060 Nishikawatsu, Matsue 690-8504, Japan*
***Department of Geology, Faculty of Science, Shinshu University, Asahi 3-1-1, Matsumoto 390-8621, Japan*
**** Department of Material Science, Interdisciplinary Faculty of Science and Engineering, Shimane University, 1060 Nishikawatsu, Matsue 690-8504, Japan*

Fe-bearing prehnite, $Ca_2Al_{2-p}Fe_pSi_3O_{10}(OH)_2$ ($Z = 2$), from Kouragahana, Shimane Peninsula, Japan, was investigated using ^{57}Fe Mössbauer spectroscopy and X-ray Rietveld method. Iron and aluminum contents of the prehnite are variable, with p ranging from 0.003 to 0.425 (n = 97). Fe-poor and Al-rich prehnites generally grow over clusters of Fe-rich prehnite crystals. Intergrowth texture of Fe-poor and Fe-rich crystals is also common in spherical aggregates. The ^{57}Fe Mössbauer spectrum consists of one doublet with isomer shift = 0.360 mm/s, quadrupole splitting = 0.276 mm/s and peak width = 0.310 mm/s. The doublet is assigned to Fe^{3+} in the octahedral site. X-ray Rietveld refinement was carried out using two structural models of space groups *Pmna* and *Pma2*. Results of the refinement are characterized by R-weighted pattern (R_{wp}) = 9.30 %, 'Goodness-of-fit' indicator (S) = 1.276 and Durbin–Watson statistic d (D–W d) of 1.485 for the refinement in space group *Pmna*, and by R_{wp} = 10.00 %, S = 1.367 and D–W d of 1.383 in space group *Pma2*, indicating that the fit of the former refinement is better than the latter. The refined Fe occupancies at the octahedral site in space groups *Pmna* and *Pma2* are 0.16 ± 0.01 and 0.20 ± 0.01, respectively. In the *Pmna*-structure, the *T2* site is occupied by $Si_{0.5}Al_{0.5}$ with disordering scheme, and average *T2*–O distance is 1.668 Å. In contrast, in the *Pma2*-structure, Al and Si are distributed in an ordered state in the *T2* site, and average Al_{T2}–O and Si_{T2}–O distances are 1.72 and 1.61 Å, respectively. Absence of Fe^{3+} from the tetrahedral site may be attributed to the small size for the cation and inflexible character of the *T2* site. A very small quadrupole splitting of the Mössbauer doublet by Fe^{3+} in the octahedral site suggests the octahedral site has a highly symmetrical site-geometry. This is consistent with a more symmetrical environment in the centrosymmetric space group *Pmna*.

Introduction

Prehnite occurs in prehnite–pumpellyite facies metamorphic rocks and in igneous rocks subjected to hydrothermal alteration. The ideal formula is $Ca_2Al(Si_3AlO_{10})(OH)_2$ ($Z = 2$) but small to moderate amount of Fe may also be present. According to single crystal structure analyses of low-Fe prehnites in the *Pncm* (Peng et al., 1959; Papike and Zoltai, 1967), *P2cm* (Preisinger, 1965; Balić Zunić et al., 1988) and *P2/n* space groups (Baur et al., 1990), prehnite has a seven-coordinated site, an octahedral site and tetrahedral *T1* and *T2* sites. The *T1* site is filled only by Si^{4+}, whereas the *T2* site is occupied by Al^{3+} and Si^{4+}. Papike and Zoltai (1967) stated that disordered arrangement of Al and Si in the *T2* site causes the centrosymmetric *Pncm* space group, whereas ordering of Al and Si produces the noncentrosymmetric *P2cm* or *P2/n* space groups. In their refinement of iron-bearing prehnite in the *Pncm* space group, Papike and Zoltai (1967) treated iron as Fe^{3+} in the octahedral site. Artioli et al. (1995) examined oxidation state and distribution of Fe in iron-bearing prehnites from low-grade metamorphosed spilitic rocks from the Keweenaw Peninsula, northern Michigan, using ^{57}Fe Mössbauer spectroscopic method, and confirmed that Fe^{3+} occurs exclusively in the octahedral site.

In their ^{57}Fe Mössbauer study of pumpellyite–okhotskite–julgoldite series minerals, Akasaka et al. (1997a) also reported the Mössbauer spectrum of prehnite coexisting with Fe-pumpellyite from gabbroic sills in Shimane Peninsula. However, the ^{57}Fe Mössbauer spectrum of their prehnite was overlapped

M. Akasaka, akasaka@riko.shimane-u.ac.jp Corresponding author
K. Makino, makinox@gipac.shinshu-u.ac.jp
R. Hino, hino@riko.shimane-u.ac.jp

by that of a small amount of Fe-bearing pumpellyite which contaminated the sample. Moreover, quadrupole splitting of the Fe^{3+}-doublet differed slightly from that of Artioli et al. (1995).

In this study, we re-examined an iron-rich prehnite from the gabbroic sills in Shimane Peninsula, and used Mössbauer method to determine the oxidation state and distribution of Fe. We also carried out X-ray Rietveld analysis of this prehnite to interpret the results of the Mössbauer analysis in terms of its structural characteristics.

Experimental methods

Sample preparation and chemical analysis

Iron-bearing prehnite has been reported from cavities of hydrothermally altered gabbroic sills in the Shimane Peninsula, Japan (Kano et al., 1986). The prehnite for our present study was collected from gabbroic sill in the Kouragahana area, Shimane Peninsula. The prehnite forms colorless to pale greenish spherical aggregates which also contain associated dark greenish Fe-rich pumpellyite and calcite. The prehnite aggregate was manually crushed down to grains 0.25 to 0.5 mm in diameter. Prehnite grains were then handpicked under a microscope and treated using dilute HCl solution to remove calcite. The purification of prehnite for the Mössbauer analysis and the Rietveld refinement was attained on these treatments, which was confirmed using X-ray powder diffraction method. Since grinding sample to very small particle sizes is one of the most critical stages of any structure study based on powder X-ray diffraction data (Bish and Reynolds, 1989; Post and Bish, 1989), the purified prehnite sample was ground finely using hand agate mortar and pestle under alcohol for about 45 minutes. The particle sizes were below 15 μm, which was examined using an optical microscope.

The chemical compositions of prehnite in the purified sample grains with 0.25 to 0.5 mm in size were analyzed using a JEOL JXA-8800 electron probe microanalyzer operated at 15 kV with beam current of 2×10^{-8} A and beam diameter of 1 μm. The ZAF method was used for data correction.

Mössbauer spectroscopy

The Mössbauer spectrum of the Kouragahana prehnite was measured at room temperature, using 370 MBeq ^{57}Co in Pd as a source. The absorber was about 100 mg of finely ground sample. Mössbauer data were obtained using a constant acceleration spectrometer fitted with a 1024 channel analyzer. Isomer shift was referred to a metallic iron foil. Doppler velocity was calibrated using the same metallic iron foil. The spectrum was fitted to Lorentzians by least-squares method with line widths and intensities constrained to be equal at each site. The QBMOSS program of Akasaka and Shinno (1992) was used for computer analysis. The quality of the fit was judged by χ^2 value and standard deviations of Mössbauer parameters.

X-ray powder diffraction

The fine powder sample was mounted in a standard aluminum sample holder with a 20 × 18 × 1.5 mm cavity. Powder was densely packed from the back of the mount against a frosted glass slide, and a flat surface level with the top of the holder was given. It is considered that specimen-displacement and transparency errors are minimized by this procedure (Raudsepp et al., 1990). According to Bish and Reynolds (1989), back-packed mounts almost completely eliminate preferred orientation in finely powdered samples which are not extremely orienting and are relatively transparent to Cu $K\alpha$ X-rays, but are not very effective at eliminating preferred orientation for materials that are notorious for orienting. Since prehnite crystals are commonly tabular parallel to {001}, such mounting method did not completely eliminate preferred orientation in this study, although it could yield mount with far less preferred orientation than conventional front-packed mount.

Step scan powder diffraction data were collected using a RIGAKU RINT automated Bragg-Brentano diffractometer system equipped with incident- and diffracted-beam Soller slits, 1° divergence and scatter slits, a 0.15 mm receiving slit and a curved graphite diffracted-beam monochromator. The Cu X-ray tube generator was operated at 35 kV and 25 mA. The profile was taken between 8° and 130° in 2θ using a step interval of 0.05° and step counting time of 3 seconds.

Rietveld structure refinement

Crystal structure of the Kouragahana prehnite was refined using the Rietveld program RIETAN-2000 (Izumi and Ikeda, 2000). The peaks were defined using a 'Modified split pseudo-Voigt' function, which comprised the split pseudo-Voigt function of Toraya (1990) combined with profile relaxation. Asymmetry parameter is build into this profile function. The details of 'Modified split pseudo-Voigt' function are described in

Izumi and Ikeda (2000). Preferred orientation was corrected with the March-Dollase function (Dollase, 1986).

Since the standard settings of the unit cell in INTERNATIONAL TABLES FOR CRYSTALLOGRAPHY published in 1989 (Bertaut, 1989) were chosen to be those of the *Pmna* and *Pma*2 space groups instead of *Pncm* and *P*2*cm*, respectively, crystal structure of the Kouragahana prehnite was here refined in the centrosymmetric space group *Pmna* and in the noncentrosymmetric space group *Pma2*. The setting in space group *Pncm* is given by changing the standard setting of **abc** in space group *Pmna* to **bca**, and the setting in space group *P*2*cm* is given by changing the standard setting of **abc** in space group *Pma*2 to $\bar{\mathbf{c}}$ **ba**. Initial structural parameters in space groups *Pmna* and *Pma*2 were taken from the single-crystal studies of prehnites of Papike and Zoltai (1967) and Preisinger (1965), respectively. Occupancies of Al and Fe^{3+} in the octahedral and tetrahedral sites were refined under the linear constraints that $g(Al) + g(Fe^{3+})$ in the octahedral site is 1.0, and $g(Al) + g(Fe^{3+})$ in the *T2* site is 0.5 in space group *Pmna* and 1.0 in space group *Pma*2, where g is the site occupancy. Nonlinear least-squares calculation using Marquardt method was followed by the conjugate-direction method to check the convergence at a local minimum (Izumi, 1993).

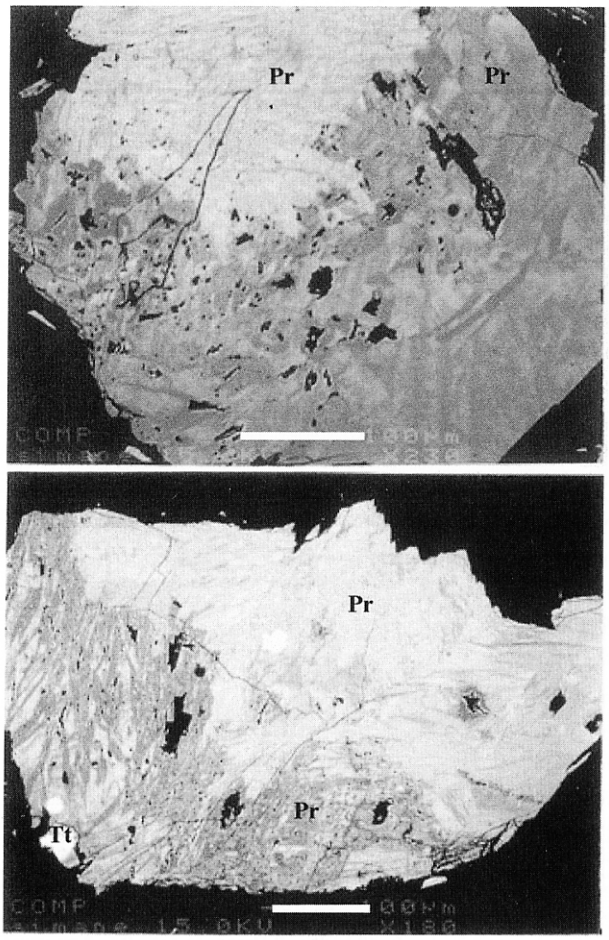

Figure 1. Backscattered electron images of Kouragahana prehnite. Abbreviation: Pr, prehnite; Tt, titanite. Scale bar is 100 μm.

Results

Chemical composition

Backscattered electron images and chemical compositions of the sample are shown in Figure 1 and Table 1, respectively. These show that iron and aluminum contents vary considerably. Fe-poor prehnite (dark gray part in Fig. 1) generally grows over clusters of Fe-rich prehnite (pale gray part in Fig. 1), or Fe-poor and Fe-rich crystals form mutual intergrowths in the spherical aggregates. As shown in Table 1, in which tri-

Table 1. Representative analyses and average composition of Kouragahana prehnite

	Minimum Fe content	Maximum Fe content	Average (n = 97)	s.d.
SiO_2	43.13	43.22	42.52	0.48
Al_2O_3	23.77	18.95	20.19	1.10
Cr_2O_3	0.00	0.00	0.02	0.02
Fe_2O_3*	0.07	8.08	5.44	1.76
MnO	0.02	0.05	0.02	0.02
MgO	0.01	0.10	0.05	0.08
CaO	26.37	26.00	26.12	0.33
BaO	0.00	0.16	0.08	0.10
SrO	0.10	0.14	0.11	0.03
Na_2O	0.00	0.03	0.02	0.02
K_2O	0.08	0.01	0.04	0.03
P_2O_5	0.05	0.04	0.02	0.03
Total	93.60	96.78	94.63	
Cations per 11 oxygens				
Si	3.025	3.021	3.014	0.009
Al	1.965	1.561	1.687	0.088
Cr	0.000	0.000	0.001	0.001
Fe^{3+}	0.003	0.425	0.290	0.094
Mn	0.001	0.003	0.001	0.001
Mg	0.001	0.011	0.005	0.009
Ca	1.982	1.947	1.984	0.021
Ba	0.000	0.004	0.002	0.003
Sr	0.004	0.006	0.005	0.006
Na	0.000	0.004	0.003	0.003
K	0.007	0.001	0.003	0.003
P	0.003	0.002	0.001	0.001
Total	6.991	6.985	6.996	

* Oxidation state of Fe was determined by Mössbauer analysis.

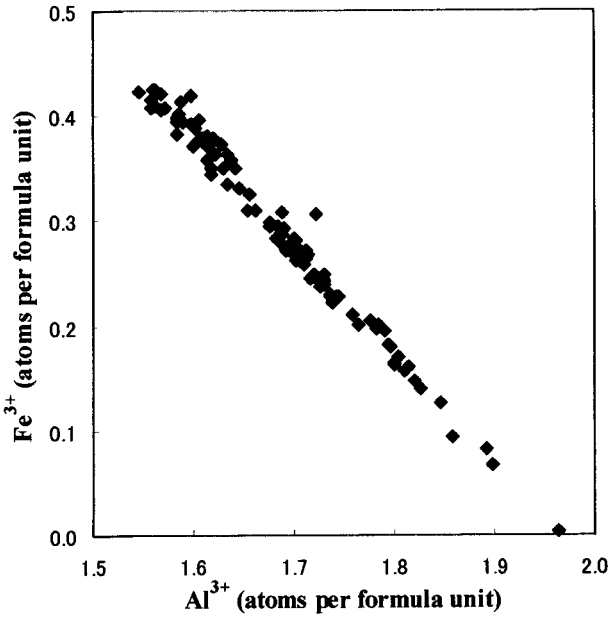

Figure 2. Al^{3+}–Fe^{3+} variation in Kouragahana prehnite.

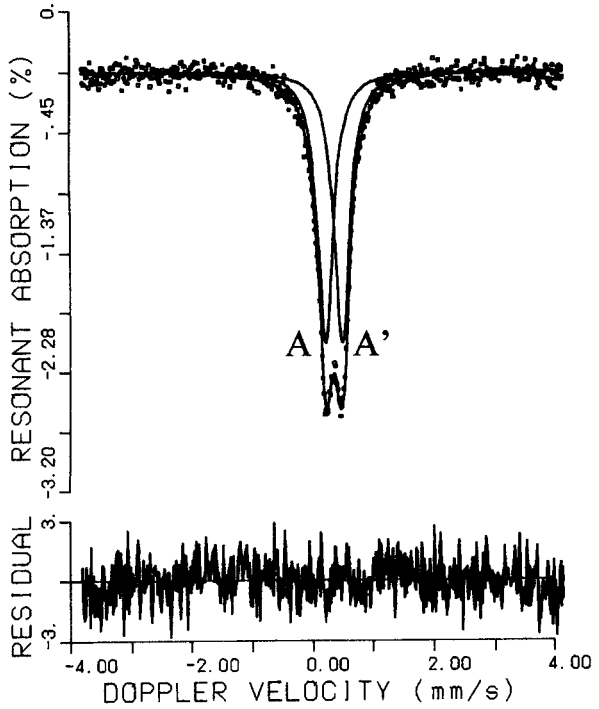

Figure 3. Mössbauer spectrum of Kouragahana prehnite. Doublet AA': Fe^{3+} in the octahedral site.

valent iron was determined by Mössbauer spectroscopic method, the chemical formula based on the average composition (n = 97) is $(Ca_{1.984}Sr_{0.005}Mg_{0.005}Na_{0.003}K_{0.003}Ba_{0.002}Mn_{0.001})_{\Sigma 2.003}(Al_{1.687}Fe^{3+}_{0.290}Cr_{0.001}P_{0.001})_{\Sigma 1.979}Si_{3.014}O_{10}(OH)_2$, although Fe^{3+} varies from 0.003 to 0.425 atoms per formula unit (a.p.f.u.). Al- and Fe^{3+}–values (a.p.f.u.) of 97 analyses are plotted on an Al^{3+}–Fe^{3+} diagram (Fig. 2) to show the distribution of analyzed data.

Table 2. Mössbauer hyperfine parameters*

	This study	Akasaka et al.(1997a)	Artioli et al. (1995)
I.S.(mm/s)	0.360(2)	0.369(8)	0.39
Q.S.(mm/s)	0.276(2)	0.274(2)	0.23
Γ(mm/s)	0.310(3)	0.320(6)	0.52
χ^2/Freedom	1.09	0.81	1.20
Assignment	Fe^{3+}_{VI}	Fe^{3+}_{VI}	Fe^{3+}_{VI}

* *I. S.*: Isomer shift referred to metallic iron absorber.
Q. S.: Quadrupole splitting.
Γ: Full width at half peak height.

Mössbauer spectroscopy

The Mössbauer spectrum and hyperfine parameters of this sample are given in Figure 3 and Table 2, respectively. The spectrum consists of one doublet that is assigned to Fe^{3+} in the octahedral site by the isomer shift

Table 3. Data collection and details of structure refinement

2θ scan range (°)	8 – 130	
Step interval (°2θ)	0.05	
Integration time/step (s)	3	
Max. intensity (counts)	5215	
No. of phase refined	1	
Space group	*Pmna*	*Pma2*
a (Å)	18.487(1)	18.487(1)
b (Å)	4.6302(3)	5.4801(3)
c (Å)	5.4802(3)	4.6306(3)
V ($Å^3$)	469.09(5)	469.14(5)
Z	2	2
D_{calc} (g/cm^3)	2.938	2.945
No. of unique reflections	846	948
No. of refined parameters	103	167
$[N-P]$*[1]	2337	2273
R_p (%)*[2]	6.59	7.35
R_{wp} (%)*[2]	9.30	10.00
R_e (%)*[2]	7.28	7.32
S*[2]	1.276	1.367
R_B (%)*[2]	2.71	2.28
R_F (%)*[2]	1.73	1.36
D–W d *[3]	1.485	1.383
r *[4]	0.762	0.765

*[1] No. of observations (steps) – no. of refined parameters
*[2] R_p: *R*-pattern, R_{wp}: *R*-weighted pattern, R_e: *R*-expected, S: Goodness-of-fit (= R_{wp}/R_e), R_B: *R*-Bragg factor, R_F: *R*-structure factor (Young, 1993)
*[3] Durbin–Watson d statistic (Hill and Flack, 1987)
*[4] Preferred-orientation parameter in the March-Dollase function

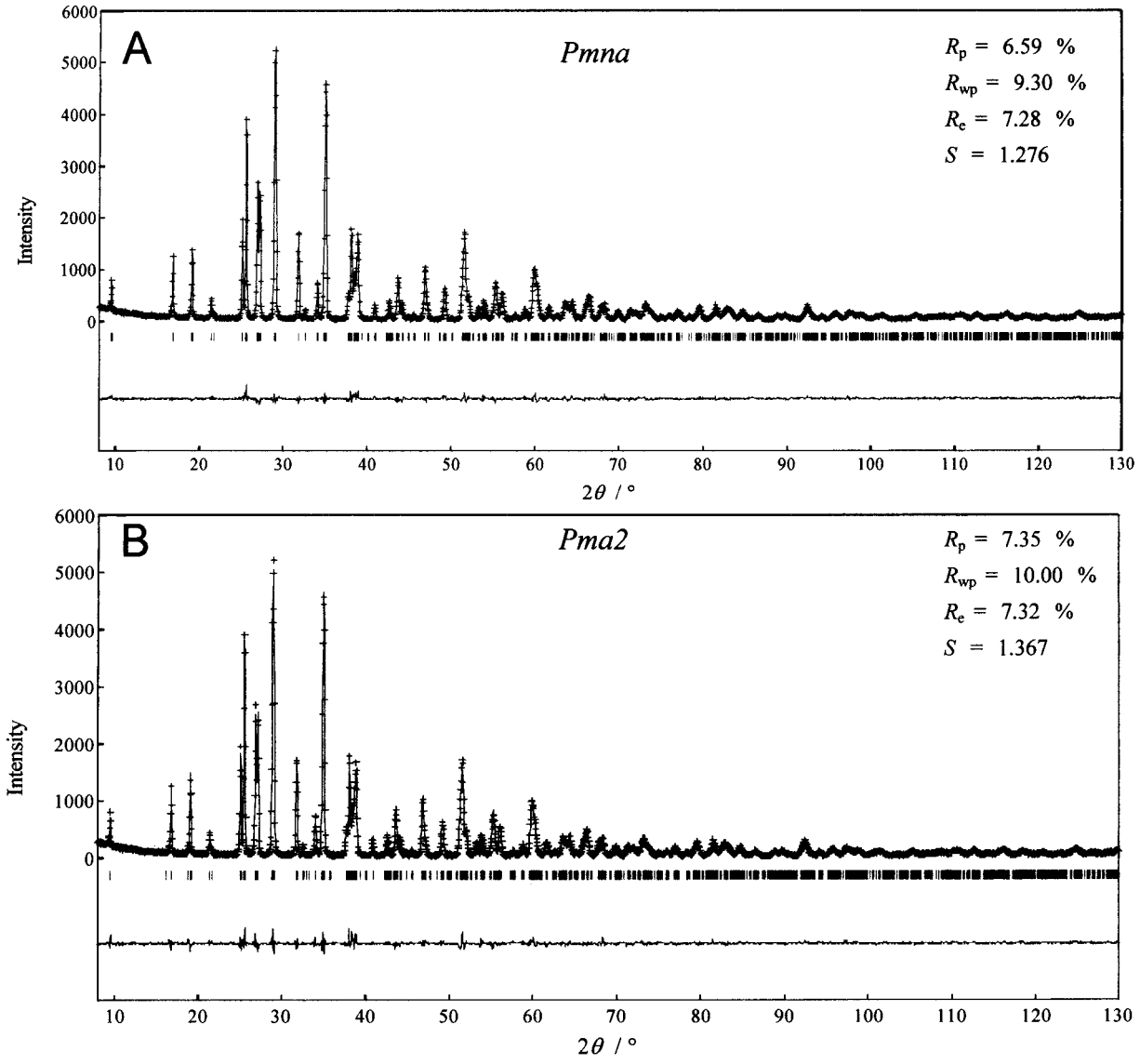

Figure 4. Observed and calculated X-ray powder diffraction patterns for Kouragahana prehnite refined in space groups *Pmna* (A) and *Pma*2 (B). The crosses are the observed data, the solid line is the calculated pattern, and the vertical bars mark all possible Bragg reflections ($K\alpha_1$ and $K\alpha_2$). The difference between the observed and calculated patterns is shown at the bottom.

(0.360 mm/s) and the quadrupole splitting (*Q.S.*) of 0.276 mm/s. The *Q.S.* value is virtually the same as the value of 0.274 mm/s reported by Akasaka et al. (1997a), and is slightly larger than the 0.23 mm/s figure of Artioli et al. (1995). These *Q.S.* values are considerably smaller than those of Fe^{3+} in the most distorted octahedral sites in other silicates such as epidote having about 2.0 mm/s *Q.S* of Fe^{3+}_{M3} (Bancroft et al., 1967; Dollase, 1973), indicating that the octahedral site in prehnite has highly symmetrical geometry.

Compared with the peak width of 0.52 mm/s reported by Artioli et al. (1995), it is notable that the peak width (0.31 mm/s) is narrow, despite the heterogeneous composition of the sample. This suggests that the crystallographic environment of the octahedral site is quite uniform.

Rietveld refinement

The refined powder patterns are shown in Figure 4. The *R*-factors (Young, 1993), 'Goodness-of-fit' indicator *S* (Young, 1993), Durbin–Watson *d* statistic (D–W *d*) (Hill and Flack, 1987) and preferred orientation parameter *r* in the March–Dollase function of the Rietveld refinement in space groups *Pmna* and *Pma2* are shown in Table 3. Refined site occupancies of Al and Fe at the

Table 4. Refined site occupancies of Al and Fe in the octahedral site, atomic positions and temperature factors

Pmna

Atom*1	Multi-plicity	Wyckoff letter	g*2	Coordinates			B*3
				x	y	z	
O(1)	8	*i*	1.00	0.0742(2)	0.744(1)	0.1341(8)	0.7(4)
O(2)	8	*i*	1.00	0.1709(2)	0.362(1)	0.2156(9)	1.4(4)
O(3)	4	*e*	1.00	0.2680(3)	0.0	0.0	1.5(4)
OH	4	*h*	1.00	0.0	0.223(2)	0.303(1)	0.1(4)
Ca	4	*e*	1.00	0.9917(9)	0.0	0.5	0.7(3)
Al	2	*a*	0.84(1)	0.0	0.0	0.0	0.5(4)
Fe	2	*a*	0.16(1)	0.0	0.0	0.0	0.5(4)
Si	4	*f*	1.00	0.1201(1)	0.5	0.0	0.8(4)
(Si,Al)*4	4	*g*	1.00	0.25	0.1901(8)	0.25	0.5(3)

Pma2

Atom*1	Multi-plicity	Wyckoff letter	g*2	Coordinates			B*5
				x	y	z	
O1	4	*d*	1.00	0.0170(3)	0.744(5)	0.021(6)	0.8(3)
O2	4	*d*	1.00	0.0728(6)	0.458(3)	0.388(5)	0.8(3)
O3	4	*d*	1.00	0.0838(6)	0.025(3)	0.656(5)	0.8(3)
O4	4	*d*	1.00	0.1797(7)	0.377(3)	0.750(5)	0.2(3)
O5	4	*d*	1.00	0.1720(7)	0.107(3)	0.256(4)	0.2(3)
OI(H)	2	*c*	1.00	0.25	0.935(4)	0.810(6)	0.2(3)
OII(H)	2	*c*	1.00	0.25	0.548(4)	0.260(6)	0.2(3)
Ca	4	*d*	1.00	0.1507(1)	0.754(2)	0.000	0.8(3)
Si1	2	*b*	1.00	0.0	0.5	0.196(5)	0.7(3)
Si2	4	*d*	1.00	0.1299(1)	0.241(2)	0.497(5)	0.7(3)
Al1	2	*a*	1.00	0.0	0.0	0.814(6)	0.6(3)
Al2	2	*c*	0.80(1)	0.25	0.261(3)	0.995(5)	0.7(3)
Fe	2	*c*	0.20(1)	0.25	0.261(3)	0.995(5)	0.7(3)

*1 Labels of atoms in space groups *Pmna* and *Pma2* are after Papike and Zoltai (1967) and Preisinger (1965), respectively.

*2 Site occupancy.

*3 Isotropic displacement parameters in Å^2.

*4 (Si,Al): $Si_{0.5}Al_{0.5}$

*5 Isotropic displace parameters in Å^2. *B*s of O1, O2 and O3 and those of O4, O5, OI(H) and OII(H) were constrained to be equal, respectively.

octahedral site, atom positional parameters and isotropic atomic displacement parameters are shown in Table 4, where labels of atoms in space groups *Pmna* and *Pma2* are after Papike and Zoltai (1967) and Preisinger (1965), respectively. Since isotropic displacement parameters (*B*s) of O3, O_I(H) and O_{II}(H) refined individually were negative in the refinement in space group *Pma2*, *B*s of O1, O2 and O3 and those of O4, O5, OI(H) and OII(H) were constrained to be equal, respectively. This indicates that the fitness of the refinement in space group *Pma2* is slightly poorer than that in space group *Pmna*, which is also shown by the Goodness-of-fit (*S*). Although the Mössbauer analysis shows that Fe^{3+} occupies only the octahedral site, we tried to refine not only the site occupancies of Al and Fe^{3+} in the octahedral site, but also those in the tetrahedral site, in order to confirm propriety of the Rietveld refinement. Since single crystal structure studies referred above indicate that the *T1* site and half of the *T2* site are filled only with Si, the site occupancies of Al and Fe in the *T2* site were refined. The present refined site occupancies in the *T2* site of the *Pmna*-prehnite were Al = 0.53 ± 0.01 and Fe = –0.03 ± 0.01, where the site occupancy of Si in the *T2* site is fixed at 0.5. In the refinement in space group *Pma2*, the *T2* site occupancies of Al and Fe were 1.01 ± 0.01 and –0.01 ± 0.01, respectively. Both results are consistent with the evidence from Mössbauer analysis that Fe^{3+} does not substitute for Al in the *T2* site. Thus, Si and Al occupancies in the tetrahedral sites were fixed to ideal values in the final refinement (Table 4).

The final results are characterized by R_{wp} (*R*-weighted pattern) = 9.30 %, S = 1.276 and D–W d of 1.485 for the refinement in space group *Pmna*, and R_{wp} = 10.00 %, S = 1.367 and D–W d of 1.383 in space group *Pma2*. Thus the fits between the observed and calculated patterns are excellent. The fit of the *Pmna*

Table 5. Interatomic distances (Å) and selected interatomic angles (°) of Kouragahana prehnite

Pmna					
Interatomic distances (Å)		Interatomic distances (Å)		Interatomic distances (Å)	
[CaO_7 polyhedron]		OH'–O(1)" (×4)	2.766(6)	O(1)–O(2) (×2)	2.556(8)
Ca–O(3)'	2.456(7)	OH'–O(1)' (×4)	2.766(6)	O(1)–O(2)' (×2)	2.667(7)
Ca–O(2) (×2)	2.644(5)	O(1)'–O(1)" (×2)	2.790(10)	[*T2*($Al_{0.5}Si_{0.5}$)O_4 tetrahedron]	
Ca–O(1)" (×2)	2.375(4)	O(1)"–O(1)"' (×2)	2.742(8)	*T2*–O(2) (×2)	1.674(5)
Ca–OH' (×2)	2.363(4)	[*T1*(Si)O_4 tetrahedron]		*T2*–O(3) (×2)	1.662(2)
Average	2.473(5)	*T1*–O(1) (×2)	1.592(5)	Average	1.668(4)
[Al*($Al_{0.84}Fe_{0.16}$)O_6 octahedron]		*T1*–O(2) (×2)	1.641(5)	O(2)–O(2)"	2.947(8)
Al*–OH' (×2)	1.956(7)	Average	1.617(5)	O(3)–O(3)'	2.820(3)
Al*–O(1)' (×4)	1.956(5)	O(1)–O(1)'	2.695(10)	O(2)–O(3) (×2)	2.724(6)
Average	1.956(6)	O(2)–O(2)'	2.688(10)	O(2)–O(3)' (×2)	2.551(6)
Interatomic angles (°)		Interatomic angles (°)		Interatomic angles (°)	
[Al*($Al_{0.84}Fe_{0.16}$)O_6 octahedron]		[*T1*(Si)O_4 tetrahedron]		O(2)–*T2*–O(3)'	99.8(2)
OH–Al*–OH'	180.0 (0)	O(1)–*T1*–O(1)'	115.6(3)	O(2)–*T2*–O(3)	109.4(2)
OH–Al*–O(1)'	90.0(2)	O(2)–*T1*–O(2)'	110.0(3)	O(3)'–*T2*–O(3)	116.0(2)
OH–Al*–O(1)"	90.0(2)	O(1)–*T1*–O(2)	104.5(2)	[*T*–O–*T*]	
O(1)'–Al*–O(1)"	91.0(2)	O(1)–*T1*–O(2)'	111.1(2)	*T1*–O(2)–*T2*	140.1(3)
O(1)'–Al*–O(1)"'	89.0(2)	[*T2*($Al_{0.5}Si_{0.5}$)O_4 tetrahedron]		*T2*–O(3)–*T2*'	157.0(4)
O(1)'–Al*–O(1)""	180.0(0)	O(2)–*T2*–O(2)"	123.5(4)	[*T*–O–Al*]	
				T1–O(1)–Al*	129.1(2)
Pma2					
Interatomic distances (Å)		Interatomic distances (Å)		Interatomic distances (Å)	
[CaO_7 polyhedron]		[Al*($Al2_{0.80}Fe_{0.20}$)O_6 octahedron]		Si2–O4	1.667(22)
Ca–O1	2.474(7)	Al*–O4 (×2)	1.838(18)	Si2–O5	1.545(23)
Ca–O2	2.817(18)	Al*–O5 (×2)	2.064(18)	Average	1.629(20)
Ca–O3	2.503(18)	Al*–OI(H)	1.986(23)	[*T2*O_4 tetrahedron]	
Ca–O4	2.431(19)	Al*–OII(H)	1.994(25)	Al1–O1 (×2)	1.727(23)
Ca–O5	2.300(21)	Average	1.964(20)	Al1–O3 (×2)	1.717(16)
Ca–OI(H)	2.264(16)	[*T1*O_4 tetrahedron]		Average	1.722(20)
Ca–OII(H)	2.471(18)	Si2–O2	1.670(17)	Si1–O1 (×2)	1.597(25)
Average	2.466(17)	Si2–O3	1.633(18)	Si1–O2 (×2)	1.631(18)
				Average	1.614(22)
Interatomic angles (°)		Interatomic angles (°)		Interatomic angles (°)	
[Al*($Al2_{0.80}Fe_{0.20}$)O_6 octahedron]		[*T1*O_4 tetrahedron]		[*T2*O_4 tetrahedron]	
O4–Al*–O4'	90.0(14)	O2–Si2–O3	108.8(4)	O1–Al1–O1'	112.6(23)
O4–Al*–O5 (×2)	90.5(3)	O2–Si2–O4	103.9 (11)	O3–Al1–O3'	129.7(17)
O4–Al*–O5' (×2)	175.7(14)	O2–Si2–O5	116.2(14)	O1–Al1–O3 (×2)	97.8(7)
O4–Al*–OI(H) (×2)	92.5(9)	O3–Si2–O4	107.1(13)	O1–Al1–O3 (×2)	109.6(7)
O4–Al*–OII(H) (×2)	96.3(9)	O3–Si2–O5	104.2(11)	O1–Si1–O1'	118.9(25)
O5–Al*–O5'	88.9(9)	O4–Si2–O5	116.2(4)	O2–Si1–O2'	113.8(16)
O5–Al*'–OI(H) (×2)	83.3(9)			O1–Si1–O2 (×2)	103.5(8)
O5–Al*–OII(H) (×2)	87.9(9)			O1–Si1–O2 (×2)	108.8(9)
OI(H)–Al*–OII(H)	167.6(15)				

See Table 4 and Figure 5 for labels of atoms.

space group is superior to that of *Pma2*. However, D–W *d* between 1.383–1.485 indicates that there is moderate positive serial correlation of the residuals, and suggests that the calculated and observed profile functions do not fully match (Hill and Flack, 1987; Hill, 1993). Compositional heterogeneity of the sample may be one reason for this.

As shown in Table 4, the refined octahedral Fe occupancies in space groups *Pmna* and *Pma2* are 0.16 and 0.20, respectively. These values are considerably lower than that given by the average EPMA composition (0.29). This suggests that the average Fe-content of the sample prepared for the X-ray Rietveld analysis was lower than that analyzed by EPMA, or that EPMA analysis positions were biased toward Fe-rich portions. The converged unit-cell parameters are similar to those previously reported (Preisinger, 1965; Papike and Zoltai, 1967; Baur et al., 1990). Interatomic distances (Å) and selected interatomic angles (°) are listed in Table 5. In Figure 5, crystal structure of the Kouragahana prehnite is projected onto the *a*–*b* and *a*–*c* planes for space groups *Pmna* and *Pma2*, respectively. In space group *Pmna*, the *T2* site is occupied by $Si_{0.5}Al_{0.5}$ and average *T2*–O distance is 1.668 Å, the same as that reported by Papike and Zoltai (1967), within error. In contrast, in space group *Pma2* Al and Si are distributed in an

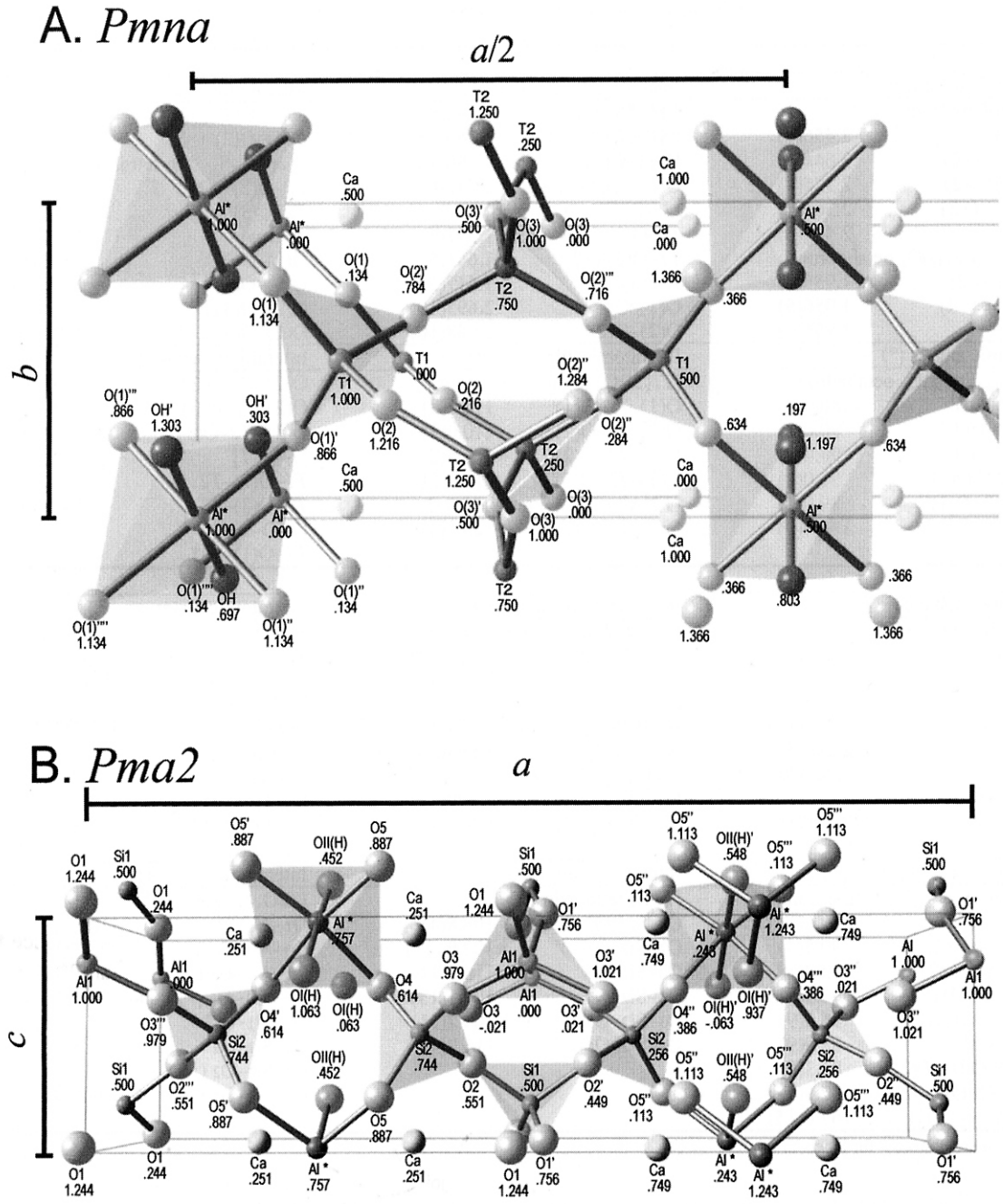

Figure 5. Projections of Kouragahana prehnite along the *c*-axis in space group *Pmna* (A) and the *b*-axis in space group *Pma*2 (B).

ordered state in the *T2* site, and average Al1–O distance (1.722 Å) is considerably larger than average Si1–O distance (1.614 Å). By the substitution of Fe^{3+} for Al in the octahedral site, average $(Al_{0.80}Fe^{3+}_{0.20})$–O distance of the octahedral site (1.964 Å) is larger than those determined by Papike and Zoltai (1967) and by Preisinger (1965), 1.92 Å.

Discussion

Aluminium is distributed in both the octahedral and tetrahedral sites in prehnite, and its space group is determined by the order-disorder scheme of Si and Al in the tetrahedral site (Papike and Zoltai, 1967). Although Papike and Zoltai (1967) refined their prehnite in space group *Pncm* with disordering state Si and Al in the *T2* site, they interpreted this structure as an average caused by an intergrowth of both *P*2*cm* and *P*2/*n* domains. Baur et al. (1990) pointed out that determination of putative Si/Al ordering and unequivocal assignment of the

proper space group is only possible by means of a full crystal structure determination, and refined orthoprehnite in space group *P2cm* and clinoprehnite in space group *P2/n*. In our study, the Kouragahana prehnite was refined in space group *Pmna* (*Pncm*), better than in space group *Pma2* (*P2cm*) in terms of the *R*-factors, *S*, D–W *d* and bond lengths. This result can be interpreted in two ways: in the Kouragahana prehnite, both Si and Al in the *T2* site are disordered, or the *Pmna*-structure is an average structure of the *P2cm* and *P2/n* domains. If we concur with the statement by Baur et al. (1990), the present X-ray powder diffraction refinement gives us no clue which interpretation is correct but the latter option seems to be more reasonable. However, as pointed out by Artioli et al. (1995), a very small quadrupole splitting of a Mössbauer doublet by octahedral Fe^{3+} suggests the octahedral site has highly symmetrical site-geometry. This is consistent with a more symmetrical environment in the centrosymmetric *Pmna* space group. Centrosymmetric orthorhombic prehnite in space group *Pmna* may be possible, not only as a hypothetical average structure, but also as a real structure.

In some Fe^{3+}-Al-bearing silicates, Fe^{3+} substitutes for Al not only in the octahedral site but also in the tetrahedral site. However, in Fe^{3+}-prehnite, confinement of Fe^{3+} to the octahedral site has been confirmed repeatedly by ^{57}Fe Mössbauer studies (Artioli et al., 1995; Akasaka et al., 1997a). In the Kouragahana prehnite, Fe^{3+} also substitutes only for Al^{3+} in the octahedral site. No substitution is observed in the tetrahedral site. The absence of Fe^{3+} in the tetrahedral site may be attributed to the small size and inflexible character of the site. In synthetic clinopyroxenes containing Tschermak's component, Fe^{3+} can occupy both the octahedral and tetrahedral sites, although the octahedral site is preferred (Huckenholz et al., 1969; Hafner and Huckenholz, 1971; Akasaka, 1983; Ghose et al., 1986; Akasaka et al., 1997b). The average *T*–O distances of synthetic $CaAlAlSiO_6$- and $CaScAlSiO_6$-pyroxenes in which the tetrahedral site is filled by $Al_{0.5}Si_{0.5}$ are 1.686 Å (Okamura et al., 1974) and 1.695 Å (Ohashi and Ii, 1978), respectively. In synthetic esseneite ($CaFe^{3+}AlSiO_6$), the average *T*–O_{brg} distance attains up to 1.713 Å by substitution of Fe^{3+} for Al in the tetrahedral site (Ghose et al., 1986). In contrast, the *T2*($Si_{0.5}Al_{0.5}$)–O distance in space group *Pmna* in prehnite is 1.668 Å (this study) or 1.674 Å (Papike and Zoltai, 1967), considerably smaller than the average *T*–O distances of the clinopyroxenes mentioned above. In the structure with space group *Pma2*, mean All–O distance in the *T2* site ranges from 1.70 Å (Preisinger, 1965) to 1.722 Å (this study), which are smaller than that in the AlO_4-tetrahedron in Tschermak-type clinopyroxenes. It seems that the limited flexibility of the *T2* site in prehnite inhibits the substitution of Fe^{3+} for Al in that site.

Conclusions

Prehnite from Kouragahana, Shimane Peninsula, contains varying amounts of Fe, ranging from 0.003 to 0.425 atoms per formula unit ($O_{10}(OH)_2$). ^{57}Fe Mössbauer and X-ray Rietveld analyses of Kouragahana prehnite indicate that Fe^{3+} is confined to the octahedral site. *T2*–O distances derived from structure refinements in space groups *Pmna* and *Pma2* suggest that the small size and limited flexibility of the *T2* site in prehnite inhibit *T2* substitution of Fe^{3+} for Al. On the basis of the single-crystal structural refinements of prehnite published to date, *Pmna*-prehnite can be interpreted to be an average structure by the *Pma2* and *P2/n* domains. However, very small quadrupole splitting of a Mössbauer doublet by Fe^{3+} suggests a highly symmetrical site-geometry of the octahedral site. This is consistent with a more symmetrical environment in the centrosymmetric space group *Pmna*.

Acknowledgements

The authors thank Professor Seiki Yamauchi of Shimane University for his help in collecting samples, Dr. Fujio Izumi of National Institute for Materials Science for his permission and help in using the Rietan-2000 program and Dr. Barry Roser of Shimane University for critical reading of the manuscript.

References

Akasaka, M. (1983) ^{57}Fe Mössbauer study of clinopyroxenes in the join $CaFe^{3+}AlSiO_6$–$CaTiAl_2O_6$. Physics and Chemistry of Minerals, 9, 205-211.

Akasaka, M., Kimura, Y., Omori, Y., Sakakibara, M., Shinno, I. and Togari, K. (1997a) ^{57}Fe Mössbauer study of pumpellyite–okhotskite–julgoldite series minerals. Mineralogy and Petrology, 61, 181-198.

Akasaka, M., Ohashi, H. and Shinno, I. (1997b) Distribution of trivalent Al, Fe and Ga ions in synthetic calcium Tschermak-type clinopyroxene. In Geochemical Studies on Synthetic and Natural Rock Systems (Gupta, A.K.et.al., Eds.). pp. 283, Allied Publishers LTD, New Delhi, 166-181.

Akasaka, M. and Shinno, I. (1992) Mössbauer spectroscopy and its recent application to silicate mineralogy. Journal of Mineralogical Society of Japan, 21, 3-20. (In Japanese with English abstract)

Artioli, G., Quartieri, S., Deriu, A. (1995) Spectroscopic data on

coexisting prehnite–pumpellyite and epidote–pumpellyite. Canadian Mineralogist, 33, 67-75.

Balić Zunić, T., Šćavničar, S and Molin, G. M. (1988) The symmetry of prehnite and the refinement of its crystal structure. Zeitschrift für Kristallographie, 185, 599 (abstract).

Bancroft, G.M., Maddock, A.G. and Burns, R.G. (1967) Applications of the Mössbauer effect to silicate mineralogy – I. Iron silicates of known crystal structure. Geochimica et Cosmochimica Acta, 31, 2219-2246.

Baur, W.H., Joswig, W. and Kassner, D. (1990) Prehnite: Structural similarity of the monoclinic and orthorhombic polymorphs and their Si/Al ordering. Journal of Solid State Chemistry, 86, 330-333.

Bertaut, E.F. (1989) Synoptic tables of space-group symbols and their use. Group-subgroup relations. In International Tables for Crystallography Volume A, Space-group symmetry Second, revised edition (Hahn T. Ed.). pp. 878, Kluwea Academic Publishers, Dordrecht/Boston/London, 47-68.

Bish, D.L. and Reynolds, R.C. (1989) Sample preparation for X-ray diffraction. In Reviews in Mineralogy Volume 20 'Modern Powder Diffraction' (Bish, D.L. and Post, J.E. Eds.). pp. 369, Mineralogical Society of America, 73-99.

Dollase, W.A. (1973) Mössbauer spectra and iron distribution in the epidote-group minerals. Zeitschrift für Kristallographie, Bd.138, S. 41-63.

Dollase, W.A. (1986) Correction of intensities for preferred orientation in powder diffractometry: application of the March model. Journal of Applied Crystallography, 19, 267-272.

Ghose, S., Okamura, F.P. and Ohashi, H. (1986) The crystal structure of $CaFe^{3+}SiAlO_6$ and the crystal chemistry of Fe^{3+} and Al^{3+} substitution in calcium Tschermak's pyroxene. Contributions to Mineralogy and Petrology, 90, 530-535.

Hafner, S.S. and Huckenholz, H.G. (1971) Mössbauer spectrum of synthetic ferri-diopside. Nature Physical Science, 233, 9-11.

Hill, R.J. (1993) Data collection strategies: fitting the experiment to the need. In The Rietveld Method (Young, R.A. Ed.). pp. 298, Oxford Science Publishing, 61-101.

Hill, R.J. and Flack, H.D. (1987) The use of the Durbin-Watson d statistic in Rietveld analysis. Journal of Applied Crystallography, 20, 356-361.

Huckenholz, H.G., Schairer, J.F. and Yoder, H.S. (1969) Synthesis and stability of ferri-diopside. Mineralogical Society of America Special Paper, 2, 163-177.

Izumi, F. (1993) Rietveld analysis programs RIETAN and PREMOS and special applications. In the Rietveld Method (Young, R.A. Ed.). pp. 298, Oxford Science Publications, 236-253.

Izumi, F. and Ikeda, T. (2000) A Rietveld-analysis program RIETAN-98 and its application to zeolites. Material Science Forum, 321-324, 198-203.

Kano, K., Satoh, H. and Bunno, M. (1986) Iron-rich pumpellyite and prehnite from the Miocene gabbroic sills of the Shimane Peninsula, Southwest Japan. Journal of Japanese Association of Mineralogy, Petrology and Economic Geology, 81, 51-58.

Ohashi, H. and Ii, N. (1978) Structure of $CaScAlSiO_6$-pyroxene. Journal of Japanese Association of Mineralogy, Petrology and Economic Geology, 73, 267-273.

Okamura, F.P., Ghose, S. and Ohashi, H. (1974) Structure and crystal chemistry of calcium Tschermak's pyroxene, $CaAlAlSiO_6$. American Mineralogist, 59, 549-557.

Papike, J.J. and Zoltai, T. (1967) Ordering of tetrahedral aluminum in prehnite, $Ca_2(Al,Fe^{3+})[Si_3AlO_{10}](OH)_2$. The American Mineralogist, 52, 974-984.

Peng, Sze-Tzung, Chou Kung-Du and Tang You-Chi (1959) The structure of prehnite. Acta Chimica Sinica, 25, 56-63.

Post, J.E. and Bish, D.L. (1989) Rietveld refinement of crystal structures using powder X-ray diffraction data. In Reviews in Mineralogy Volume 20 'Modern Powder Diffraction' (Bish, D.L. and Post, J.E. Eds.). pp. 369, Mineralogical Society of America, 73-99.

Preisinger, A. (1965) Prehnit–ein neuer Schichtsilikattyp. Tschermaks Mineralogische und Petrographische Mitteilungen, 10, 491-504.

Raudsepp, M., Hawthorne, F.C. and Turnock, A.C. (1990) Evaluation of the Rietveld method for the characterization of fine-grained products of mineral synthesis: the diopside–hedenbergite join. Canadian Mineralogist, 28, 93-109.

Toraya, H. (1990) Array-type universal profile function for powder pattern fitting. Journal of Applied Crystallography, 23, 485-491.

Young, R.A. (1993) Introduction to the Rietveld method. In the Rietveld Method (Young, R.A. Ed.). pp. 298, Oxford Science Publications, 1-38.

Manuscript received; 2 December, 2002
Manuscript accepted; 25 February, 2003